ingegneria sismica
International Journal of Earthquake Engineering
Anno XLIII - Num. 2 - 2026

Thermal Runaway Spread and Quantity Assessment of Electric Vehicles Carried by Rolling Stock Vessels Based on Fire Dynamics Simulation

Pan Shao[1,*], *Daowang Ren*[2] *and Guoqi Ma*[3]

[1] China Waterborne Transport Research Institute Beijing 100088, Beijing, China
[2] Shandong Gangtong Engineering Consulting Co., Ltd, Yantai 264000, Shandong, China
[3] Rizhao Transportation Bureau, Rizhao 276800, Shandong ,China

SUMMARY: *As electric vehicles (EVs) have become increasingly widespread, the danger of fires stemming from the transportation of EVs on passenger roll-on/roll-off (PRO) ships has grown notably more significant. The article takes a 15000GT passenger ship as the research object, and uses FDS numerical simulation software to establish a fire simulation model for the transportation of electric vehicles on the passenger ship, and realizes the simulation and simulation analysis of the thermal runaway of electric vehicles. Subsequently, the YOLOv5 model was integrated with the attention mechanism to develop the YOLOv5 - ECA model. This newly - developed model is intended for assessing the quantity of targets at the fire scene of an electric vehicle transported on a passenger - roller ship. The results show that the PHRR of EVs in a fire can reach up to 29.75 MW in 600 s, which is only 0.84% different from the actual calculation results. The YOLOv5-ECA model achieves a mAP of 88.42% for EV target number detection, and the overall model volume is lower and the detection speed is faster. Therefore, relying on the effective combination of fire dynamics simulation and deep learning technology, the analysis of thermal runaway spread of electric vehicles carried by passenger ships can be realized, and the possible economic losses of electric vehicles under fire scenarios can be more accurately grasped to provide guidance for good fire prevention measures.*

KEYWORDS: *FDS numerical simulation; attention mechanism; YOLOv5-ECA model; passenger roll-on/roll-off ship; electric vehicle; fire simulation model*

1 Introduction

The overwhelming majority of electric cars are energized by lithium - ion batteries, and since their introduction, fires due to charging fires, collision fires, and spontaneous combustion have occurred from time to time, causing public concern about the safety of electric vehicles [1, 2].Particularly in the past few years, numerous fire incidents have taken place on passenger ships and roll-on/roll-off vessels transporting electric vehicles. The safety hazard has grown more and more conspicuous, presenting novel challenges to the shipping sector and regulatory bodies[3, 4]. Numerous fire cases and tests have proved that fires caused by lithium batteries are characterized by strong thermal runaway concealment, rapid temperature rise, fast heat spread, anaerobic combustion, easy to rekindle, etc., which, superimposed on the safety requirements of passenger-roller ships, bring great challenges to the emergency disposal of ship fires [5-7].

*cxsp19860717@126.com
https://doi.org/10.65102/is2026614
Published: 30 April, 2026

Currently, the phenomenon of fires caused by electric vehicles carried by passenger-roller ships has received widespread attention. Reference [8] stressed that as the utilization of electric vehicles rises, the fire incidents they cause have drawn people's attention. It detailed the fires caused by electric vehicles on passenger - roll ships, conducted tests on fire occurrences in internal - combustion - engine electric vehicles and pure electric vehicles, and proposed countermeasures.Reference [9] pinpoints the fire hazards related to the transportation of electric vehicles on roll - on/roll - off vessels. This is primarily because these vehicles are powered by lithium batteries. Currently, these fire hazards are an escalating concern, and specific safety measures must be put into practice.Reference [10] stated that as the quantity of electric vehicles increases, the accidents stemming from the transportation of electric vehicles via roll - on/roll - off vessels have led to substantial losses for the industry,and based on a database analysis revealed that the main causes of their accidents are fires or explosions, and proposed countermeasures to reduce the risks. Literature [11] aimed to identify the main risks of ship cargo and electric vehicles in maritime transportation, based on a questionnaire survey that showed that overheating and battery fires are the most significant risk factors, which occur more frequently than other risks, Moreover, it is essential to evaluate the efficacy of risk mitigation strategies. In literature [12], it is reported that the quantity of electric vehicles transported by passenger roll - on/roll - off ships has been steadily rising. The occurrence of electric vehicle fires within the enclosed areas of these ships has given rise to significant safety apprehensions. To address this, vehicle zoning parking strategies are put forward to alleviate the impact of fires on passenger roll - on/roll - off ships.Literature [13] delved into the fire risks associated with electric vehicles on passenger roll - on/roll - off vessels. It investigated the probabilistic features of the primary fire hazards in the enclosed spaces to ascertain their importance in the occurrence of fires on such vessels. Based on this analysis, effective countermeasures were proposed.Literature [14] highlighted that the escalating demand for electric vehicles has led to an increased incidence of fire risk on passenger roll - on/roll - off vessels. By scrutinizing the fire incidents on these vessels, it was recognized that there is a need for better management of the vehicle cargo's condition, a more effective response from the fixed fire suppression system, and more comprehensive system inspections.

In fire research, the experimental methodological aspects of the study have a considerable importance, relying on advanced testing means and instruments can directly record the spatial distribution and changes over time of important parameters in the fire spreading process [15, 16]. However, due to the uncertainty of fire and the destructive nature of fire experiments, there are many challenges in experimental research. In the wake of the swift advancement of computer science, fire dynamics simulation has been rapidly developed on the basis of existing experiments, Integrated with certain fundamental theories like combustion, heat exchange, and computational fluid mechanics [17, 18]. It uses computer technology to numerically simulate and predict the flame pattern, smoke emission and heat field distribution when a fire occurs, which can help firefighters make more accurate judgments and decisions at the fire scene and improve the efficiency and quality of firefighting work [19-22]. Compared with experimental means fire dynamics simulation has the characteristics of less cost, flexible simulation conditions, and high repeatability. Regarding the application of fire dynamics simulation in fire prediction, literature [23] discusses the application of fire dynamics simulation in building fires, Fire dynamics simulation can offer solutions to halt the spread of a fire. It does this by examining the fire's development time, its level of hazard, the temperature it reaches, and the visibility conditions associated with it. Literature [24] describes the spread of fires in hospitals and proposes the application of fire dynamics simulation, which is able to find effective fire management measures by analyzing the fire situation, smoke layer flow, building structure, fire

fighting equipment, and other factors. Literature [25] emphasized the seriousness of building fires and explored the effectiveness of a tool constructed based on fire dynamics simulation in reducing fire hazards, Demonstrating that it offers a more all - encompassing evaluation of evacuation performance when contrasted with the current safety protocols in the industry. Literature [26] investigated issues related to the simulation of cinema fires by fire dynamics simulators and verified that fire dynamics simulators are able to capture the main trends in smoke dispersion, thus realistically predicting the associated safety risks.

At present, the fire dynamics simulation technology has reached a high level of maturity. It can numerically model the thermal runaway propagation and quantity estimation of electric vehicles on passenger roll - on/roll - off ships, among other situations. This technology also offers dependable predictions of fire spread and fire - extinguishing scenarios [27, 28]. In this context, the literature [29] stressed that passenger and roll - on/roll - off vessels transporting electric vehicles present numerous difficulties for fire safety management. It put forward the use of fire dynamics simulation tools. These tools can forecast the temperature during an accident, thereby lessening fire - related damage. The literature [30] identified the potential fire risks associated with electric vehicles on passenger and roll - on/roll - off ships. To mitigate the harm, a fire dynamics simulator program was employed to simulate the fire propagation process. This highlighted the efficacy of the method, which can minimize the spread of smoke.

The conveyance of electric vehicles on passenger roll-on/roll-off ships serves as a crucial safeguard for the further advancement of eco - friendly development. However, there exists a potential fire hazard during the transportation phase. In this research, a fire dynamics simulation approach is employed to simulate and analyze the propagation of thermal runaway in electric vehicles transported by passenger and roll - on/roll - off vessels. Moreover, a deep learning technology is incorporated to aid in achieving the target detection of the quantity of electric vehicles damaged in a fire situation. This study proposes a new research perspective to determine to achieve the quantity assessment of electric vehicles, which can better promote the optimization of fire prevention measures for electric vehicles carried on passenger and roll-on/roll-off vessels.

2 Modeling of the fire dynamics of electric vehicles transported on roll-on/roll-off passenger vessels

Roll-on/roll-off (Ro-Ro) vessels are ships used to carry passengers, vehicles and cargoes, and have a competitive advantage in short- and medium-distance water transportation between inland seas, bays, straits and coastal islands. As the electric vehicle market experiences swift expansion, the transportation of electric vehicles using roll - on/roll - off ships is steadily increasing. In the context of electric vehicle transportation on passenger - roll ferries, there is a heightened risk. This is because of the combustion properties of electric vehicle batteries. Neither the fixed gas fire - suppression system nor the water - spray fire - suppression system can function effectively. Consequently, it is more challenging to handle fire emergencies during the voyage of passenger - roll ferries that carry electric vehicles.

2.1 Numerical simulation software and fire dynamics theory

2.1.1 FDS numerical simulation software

FDS is a field - based model fire simulation program created by NIST. It makes use of the Large Eddy Simulation (LES) method,which assumes that the eddies in a fire-generated gas mixture are sufficiently large in size and slow in motion to be able to solve the equations with reasonably

acceptable accuracy by virtue of the hydrodynamic equations and to roughly account for, or ignore, small-scale eddy motion.

Pyrosim is a software for firefighting simulation. Pyrosim provides an integrated development environment for FDS software that merges commonly used tools into a graphical user interface. Pyrosim can not only construct building models directly through the graphical user interface, but also import common 2D drawing files or 3D models, including BIM models in IFC format, DWG supported by Autodesk CAD and so on. This process gives the researcher the ability to quickly build complex fire scenarios compared to the code that needs to be employed for modeling when FDS is used directly. In addition, for the input of fire parameters Pyrosim provides a windowed interface, but at the same time FDS commands can be used for the input of fire parameters.

Generally, the process of conducting a fire simulation involves three primary steps as follows:

(1) Create the FDS computational model. This step is mainly for dividing the network in the software, determining the parameters of combustibles and obstacles, defining the surface layer, modeling the fire obstacles (mainly building contours), defining the point of origin, vents, etc., and completing the entity parameter settings of an FDS model.

(2) FDS simulation parameter setting. This step is mainly to determine the entire fire simulation duration, simulation output parameters, simulation mode, simulation of the external environment and other parameters in the software, to complete the FDS model of the operation of the simulation parameters set.

(3) Calculation and result analysis. This step is mainly to call the FDS simulator through Pyrosim to carry out calculations and interpret the simulation, and the FDS simulation results can be viewed through the Smokeview sub-software for four-dimensional visualization, including smoke data, fire source data, and cloud maps of the preset locations. In addition, a range of fire-related physical values can be exported, including temperature and gas concentrations at predefined points.

2.1.2 Theoretical knowledge of fire dynamics

In the actual process of various fires, although the various state parameters of the smoke, such as temperature, component concentration and velocity changes with time and space, but the rule of law should still meet the general combustion and flow laws. Therefore, some of the most basic principles and methods can be considered to describe the velocity field, concentration field and temperature field changes, which is the field simulation. That is,The setup area is partitioned into numerous small three - dimensional rectangular control volumes or computational cells. In each of these cells, the density, speed, temperature, pressure, and component concentration of the gas are computed.Drawing on the widely - recognized principles of mass conservation, momentum conservation, energy conservation, and the laws of chemical reactions, a series of fundamental equations are derived through mathematical abstraction. This set of equations includes the continuity equation, the momentum equation, the energy equation, the component equations, and several auxiliary equations. These equations are presented in the form of partial differential equations and approximated using finite differences.The finite volume method is employed on the same mesh for multiple purposes. It is used to calculate thermal radiation. Given the occurrence of turbulent flow in the fluid, it helps in tracking and forecasting the generation and movement of fire - related gases. Additionally, by integrating with the properties of materials, it can be used to calculate the development and propagation of a fire.

The large eddy numerical simulation method in FDS software, which is commonly used nowadays,It is employed to concentrate on the computation of the smoke and heat transfer

procedure during a fire, encompassing the alterations in the distribution of the burning rate, temperature, visibility, and so on. The basic conservation equations of the LES numerical simulation algorithm mainly include the continuity equation, the equations such as the momentum equation, the energy equation, the component equations, the equation of state, and the chemical reaction equations are presented as follows. :

The equation of continuity can be formulated as:

$$\frac{\partial \rho}{\partial t} + \nabla \left| \cdot \rho u = 0 \right. \tag{1}$$

The momentum equation is expressed as:

$$\rho \left(\frac{\partial u}{\partial t} + (u \cdot \nabla) u \right) + \nabla p = \rho g + f + \nabla \cdot \tau \tag{2}$$

The energy equation is expressed as:

$$\frac{\partial}{\partial t}(\rho h) + \nabla \cdot \rho h u = \left(\frac{Dp}{Dt} - \nabla \cdot q_r \right) + \nabla \cdot k \nabla T + \sum_L \nabla \cdot h_{t_p} D_t \nabla Y_t \partial \tag{3}$$

The component equations are expressed as:

$$\frac{\partial}{\partial t}(\rho Y_t) + \nabla \cdot \rho Y_t u = \nabla \cdot \rho D_t \nabla Y_t + \dot{m}_t^m \tag{4}$$

The equation of state (auxiliary equation) is expressed as:

$$p_0 = \rho R T / M \tag{5}$$

The chemical reaction equation is expressed as:

$$C_x H_y O_z + v_{O_2} O_2 \rightarrow v_{CO_2} CO_2 + v_{H_2O} H_2O + v_{CO} CO + v_{Soot} Soot \tag{6}$$

$$S = C / \left(K_m \rho Y_S \right) \tag{7}$$

where t denotes time, T denotes temperature, p denotes density, $Soot$ denotes soot, S denotes visibility, and Y_S denotes smoke concentration.

The above equations are combined to calculate and simulate the change of combustion rate, temperature, visibility and other indicators when the fire occurs Within the passenger ship, there is an electric vehicle being transported.

2.2 A fire simulation model for the deck of a roll - on/roll - off passenger vessel transporting electric cars

2.2.1 Electric Vehicle Deck Model for Rolling Stock Vessels

In this paper, the 15000GT roll-on/roll-off passenger ship is taken as the research sample, whose overall length and the length between two columns are 137.5m and 127.6m, The width and depth of the type measure 23.5 meters and 8.5 meters, correspondingly. Meanwhile, the design

draft and the structural draft are 5.5 meters and 6.0 meters, respectively. respectively, and the loading capacity is about 240 vehicles, with the overall speed of about 18kn, the range of 2,400n mile, and the main engine power designed to be 2 *6000kW*600r/min.

The ship is double engine with double adjustable oars, double rudders, bulbous nose bow, square stern, and is equipped with bow-side push, sway-reducing fins and anti-transverse tilting device. The vessel has multi-level continuous decks, with the engine pump compartment located at the stern. Electric vehicles are mounted on the first and third decks, with vehicle loading and unloading accessed through a tailgate on the aft end of the third deck (upper cargo hold), and access to the first deck (lower cargo hold) through a fixed ramp located on the starboard side of the aft end. Passenger and crew areas are arranged on decks five to eight. The middle part of the fifth deck is mainly arranged with passenger entrance hall, service desk, mini-market and third and fourth class cabins, while the aft part is arranged with general crew living area. The sixth deck is mainly arranged with passenger and crew dining room, bar, multifunctional entertainment hall and other public cabins, and the first part is arranged with second and third class cabins. The seventh deck is primarily designated for cabins of the first, second, and third classes. At the rear of the ship, the first - class cabins are situated. Meanwhile, the eighth deck is allocated for the bridge and the living quarters of the senior crew.

2.2.2 Fire Simulation Model for Electric Vehicles on Rolling Stock Vessels

Simplified according to the actual cabin data of 15000GT class passenger roll-on/roll-off ship, the deck of the passenger roll-on/roll-off ship carrying electric vehicles is set to be 110.0m long, 25.0m wide and 5.0m high.Since the thickness of the deck is 14.0mm, which is much smaller than the unit data of the grid (0.4m×0.4m×0.4m), the thickness of the deck can be ignored. The material of the deck is steel and can be set as steel in the grid i.e. deck. There are 240 cars distributed in the three electric car decks, which is in accordance with the code. The lane width is set to 2.5 m. The vehicle spacing is 0.25 m from left to right and 1.6 m from front to back.The four stairway openings of the EV deck model are located on the upper deck of the EV deck and are symmetrical from left to right, with a length of 4.2 m and a width of 2.4 m. The stairway openings of the EV deck model are located on the upper deck of the EV deck and are symmetrical from left to right.

Taking the conservative most unfavorable principle as the fire scenario design principle, 3 fire sources are set in the center position of the electric car deck of the passenger-roller ship carrier, and its simplified model is shown in Fig. 1 (which only represents 148 electric cars on one deck). The vehicle in the middle position firstly catches fire and ignites the vehicles on the left and right sides, so as to analyze the spreading state, temperature field change and visibility distribution of the smoke generated on the car deck, i.e., the middle vehicle is the initial source of fire, and the other two are delayed sources of fire, which catch fire after a delay of 100 s. The t2 fire source model is employed to conduct an analysis of the fire source on the car deck. When the t2 fire source model is utilized for this analysis, it is found that the fire type of the vehicles on the deck of a passenger - roll - on/roll - off ship that carries electric cars falls into the category of ultra - rapid fire. This type of fire corresponds to a fire growth coefficient of 0.1872 kilowatts per second squared.

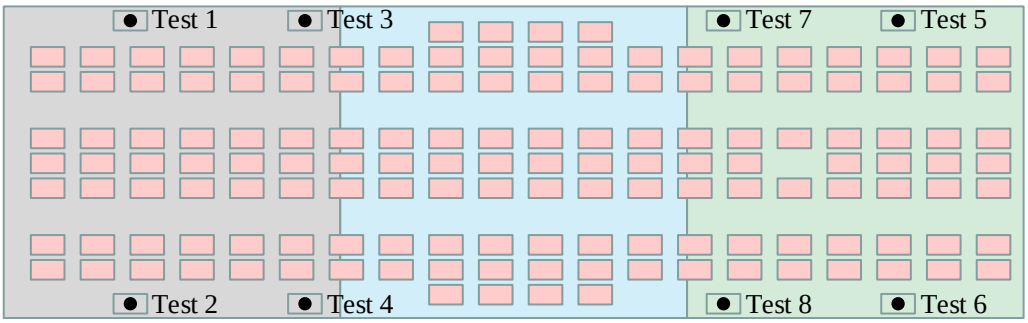

Figure 1: The passenger roller carries electric car fire simulation model

Grid local encryption is set up in FDS, the middle grid of the fire source location is 0.4m×0.4m×0.4m, and the left and right sides are 0.9m×0.9m×0.9m, which get the total number of grids of 100,000, the number of grids in the middle is 70,000, and the number of grids in the left and right sides are all divided into 10,000. The ventilation is set up to be natural ventilation, without mechanical ventilation facilities. The data monitoring setup is the monitoring of 8 stairwells (Test1~Test8) in a horizontal section of 1.5m in height with the EV deck leading to the upper space, and the temperature and smoke concentration data are monitored, respectively.

2.2.3 Calculation of the size of fires on passenger ships carrying electric vehicles

The rate at which heat is released during a fire, known as the heat release rate (HRR), stands as a crucial metric for gauging the magnitude of a fire. The heat release rate refers to the quantity of heat liberated from the combustion of combustible substances within a given time frame under well - defined test circumstances.This rate is closely associated with two key factors: the rate at which the material burns in terms of mass and the material's heat of combustion. The heat release rate significantly impacts both the fire itself and the volume of smoke generated.Mathematically, the heat release rate can be presented as follows:

$$Q_{HRR} = \dot{m}\Delta H_e = A_f \dot{m}''\eta\Delta H_c \tag{8}$$

where $\dot{m}$ is the rate of combustion, which can be measured by the rate of mass loss during the test, ΔH_e is the effective heat of combustion, A_f is the floor/surface area of the fuel or fire, and $\dot{m}''$ is the rate of combustion of the fuel per unit area. η depends on the combustion efficiency of the oxygen supply, and ΔH_c is the heat of combustion of the EV battery, This parameter, which depends on the kind of lithium - ion battery and the state of charge (SOC), shows variation.

For electric vehicles, the main combustible in the powertrain is the power battery. Consequently, the heat release rate of an electric vehicle can be partitioned into two segments: that of the power battery and that of other flammable materials. When taking the most adverse situation into account, the peak heat release rate (PHRR) is regarded as the total of the peak heat release rates of all flammable substances in an electric vehicle that is ablaze with a roaring ignition. The details are as follows:

The maximum rate of heat release of different types of lithium batteries has a linear relationship with the 0.6 power of its battery capacity E_B, which applies to a range of about $10\,\text{Wh}$ to $10^7\,\text{Wh}$, i.e., from single lithium batteries to large-scale lithium battery storage devices, with the relationship equation:

$$Q_{PHRR} = 2E_B^{0.6} \tag{9}$$

The peak heat release rate of the power battery can be estimated on the basis of the energy capacity of the power battery of the pure electric vehicle through equation (2).

Other common combustibles in pure electric vehicles include different types of plastics and leather, nonwoven fabrics, etc. The difference in peak heat release rate between different materials may be large.

At a thermal radiation intensity of $45\ \mathrm{kW/m^2}$, PVC leather-nonwoven felt has the highest peak heat release rate per unit area, which can reach $\dot{q}'' = 438.42\ \mathrm{kW/m^2}$. The following formula can be used to estimate the peak heat release rate of other combustibles in a pure electric vehicle fire. i.e:

$$Q_{PHRR} = \eta A_f \dot{q}'' \tag{10}$$

where $\dot{q}''$ is the peak combustion rate per unit area, η is the combustion efficiency, and A_f is the combustion area.

Combined with equations (9) and (10) can be estimated peak heat release rate during fire. i.e:

$$Q_{PHRR} = \frac{2E_B^{0.6}}{1000} + \eta A_f \dot{q}'' \tag{11}$$

3 Target number detection for electric vehicles based on YOLOv5-ECA

Roll-on/roll-off transportation of passengers and cargo is a very important mode of transportation, and plays an irreplaceable role in safeguarding people's livelihood in places such as the Qiongzhou Strait. As the electric vehicle sector undergoes consistent and swift advancement, a greater number of electric cars will find their way into numerous households. Consequently, the conveyance of electric vehicles via roll-on/roll-off passenger vessels is set to become increasingly prevalent. However, In the event that a fire breaks out while electric vehicles are being transported via roll - on/roll - off ships, how to effectively realize the detection of electric vehicle combustion and quantity assessment has become an important method to reduce the loss of electric vehicles.

3.1 YOLOv5 target detection model and attention mechanism

3.1.1 YOLOv5 target detection model

Inspired by CSPNet, YOLOv5 designs CSPDarkNet as the backbone network.The CSPNet model divides the input feature maps into two parts, where one part of the feature maps will be processed by the convolution operation, while the other part passes through and outputs from the dense blocks and the transition layer, and finally the two outputs are subjected to the concat operation.YOLOv5 borrows the CSPNet to propose the CSP structure. Figure 2 shows the framework of CSP module, there are two main types, CSP1 finds its application in the backbone network, while CSP2 is utilized in the feature fusion segment. The CSP module proficiently addresses the issue of gradient vanishing that arises due to the network's deepening.

Simultaneously, as the Backbone network becomes deeper, the feature granularity acquired via the CSP module becomes finer. This, in turn, further enhances the network's feature extraction capability.

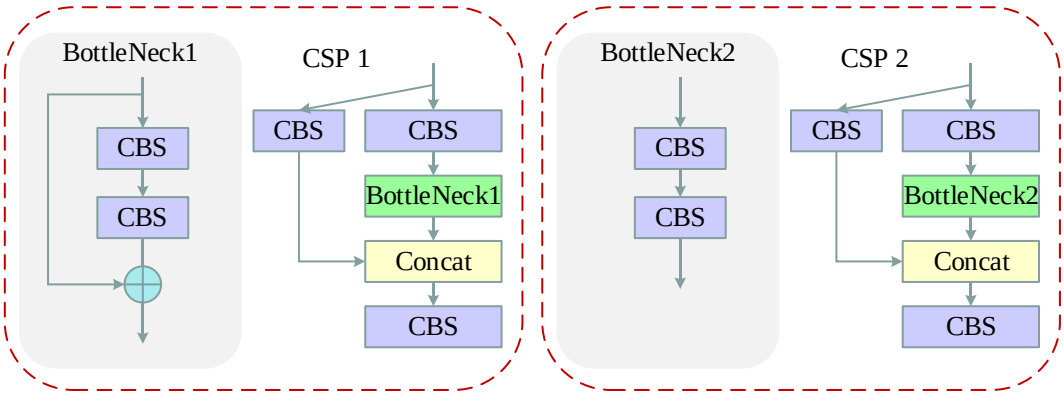

Figure 2: CSP module structure diagram

YOLOv5 also adds the first Focus structure at the front end, the core part of which is the slicing operation. If the input image of Focus is 640*640*3, then after slicing, the output result will become 320*320*12. The Focus module optimizes the normal convolution operation, and downsampling in this way can effectively reduce the number of parameters and thus increase the speed, and the basic target information of the processed feature maps is not lost, but only the spatial information will be transformed into the channel information. The fundamental target details of the processed feature map remain intact. However, the spatial data is converted into channel - related data, leading to an augmentation of the feature map's channel dimension.

The output constitutes the final detection segment. The forward architecture of the YOLOv5 network makes use of three top - down convolutional layers for detecting objects of varying sizes. The dimensions of these three outputs are four, eight, and sixteen times the size of the input image respectively. Given that the size of the feature map is inversely proportional to the perceived object size, small feature maps are employed to detect large objects, while large feature maps are used for detecting smaller objects. .

3.1.2 Attention mechanisms

The attention mechanism is a method that works by giving higher weights to important information in an image and ignoring less relevant information. It has the ability to dynamically adjust the weights to accommodate the selection of important information in different situations, thus making the model highly scalable and robust. In fire scenarios, Owing to the existence of a substantial quantity of smoke the attention mechanism can be utilized to assign weights to the information in the image in order to focus more on the key information such as electric cars and ignore other complex information. By adopting this approach, the precision and functionality of target detection can be improved so that the model is more focused on focusing on important targets such as the number of electric cars burning.

The channel attention mechanism (CA) utilizes the relationship between channels within the feature map to generate a channel attention feature map. Within the feature map, every channel can be regarded as a feature identifier. Thus, the objective of the channel attention mechanism is to pinpoint the channels that contain valuable information within the image. The equation for the channel attention mechanism is:

$$\begin{aligned} M_c(F) &= \sigma\left(MLP\left(AvgPool\left(F\right)\right) + MLP\left(MaxPool\left(F\right)\right)\right) \\ &= \sigma\left(W_1\left(W_0\left(F_{avg}^c\right)\right) + W_1\left(W_0\left(F_{\max}^c\right)\right)\right) \end{aligned} \tag{12}$$

By leveraging the spatial attention mechanism (SA), the model is capable of exploiting the inter - relationships among the internal spaces of the feature maps. This enables the generation of a spatial attention feature map, which zeroes in on the position of relevant information within the feature map. In the spatial attention mechanism, two operations - average pooling and maximum pooling - are carried out on the feature maps along the channel dimension. Subsequently, the feature maps produced from these operations are concatenated. After that, convolution operations are applied to the concatenated feature maps to yield the ultimate spatial attention feature maps. The mathematical formula for the spatial attention mechanism is presented as:

$$\begin{aligned} M_s(F) &= \sigma\left(f^{7\times7}\left(\left[AvgPool\left(F\right); MaxPool\left(F\right)\right]\right)\right) \\ &= \sigma\left(f^{7\times7}\left(\left[F_{avg}^s; f_{\max}^s\right]\right)\right) \end{aligned} \tag{13}$$

In the event of a fire on a passenger ship transporting electric vehicles, a high degree of precision is necessary for the detection of electric vehicles to attain the objective of assessing the quantity of electric vehicles. To this end, the attention mechanism is incorporated into the backbone feature extraction network. This enables the network to extract a greater amount of feature - related information during the feature extraction phase. As a result, during the feature fusion process, the extracted feature information can be more effectively integrated, thereby enhancing the accuracy of traffic sign detection.

3.2 Improvement of YOLOv5-ECA target detection model

3.2.1 YOLOv5-ECA model architecture

To make it suitable for the task of detecting small targets like electric vehicles transported by passenger and roll - on/roll - off ships, this paper presents the YOLOv5 - ECA architecture, as depicted in Fig. 3. Based on the YOLOv5 framework, the coordinate attention mechanism (ECA) is incorporated. This mechanism not only prevents degradation and cross - channel interaction to uphold the model's performance but also substantially decreases the model's complexity and enhances the feature extraction capability.Next, the model's capacity to detect minuscule targets is enhanced by adding a small - scale detection layer. Finally, in the backbone network, BSConv is employed in place of regular convolution to cut down on the model's parameters.

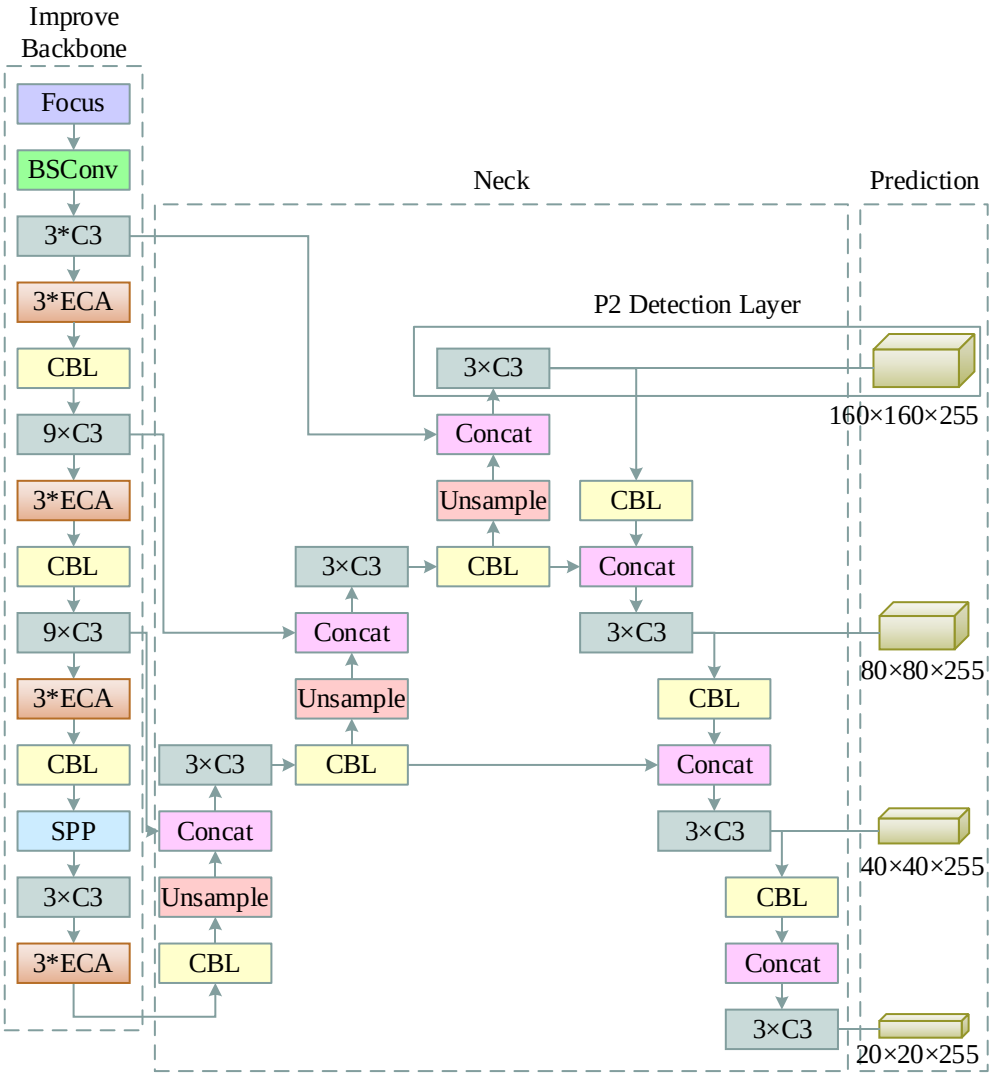

Figure 3: YOLOv5-ECA model architecture

3.2.2 Integration of coordinate attention mechanisms

The coordinate attention mechanism is a type of attention mechanism that generates accurate positional perception. It can perceive positions in the spatial direction, allowing the network to focus on a broader area. The coordinate attention mechanism takes into consideration both the relationship among feature channels and the location data to more effectively localize sensitive regions.This mechanism primarily comprises two components: coordinate information embedding and coordinate attention generation. These components are used to establish the long - range dependency on the target, as described below:

(1) Coordinate information embedding

Different from using 2D global pooling to calculate the channel attention, the coordinate attention mechanism divides the two - dimensional global pooling into two one - dimensional encoding operations. Through these operations, it acquires the positional data from the horizontal and vertical orientations respectively. .

Specifically a pair of pooling kernels of dimensions $(H,1)$ and $(1,W)$ are used to encode features in horizontal and vertical directions for each channel of the input features to obtain perceptual features in both directions, computed under the following procedure:

$$z_c^h(h) = \frac{1}{W} \sum_{0 \le i < W} P_c(h, i) \tag{14}$$

$$z_c^w(\omega) = \frac{1}{H} \sum_{0 \le j < H} P_c(j, \omega) \tag{15}$$

where z_c^h denotes the perceived features in the vertical direction, z_c^w denotes the perceived features in the horizontal direction, P_c denotes the input features from the upper network, and the subscript c is the channel to which the feature vector belongs.

(2) Coordinate Attention Generation

After obtaining the perceptual features, the channel information can be encoded. When encoding, the perceptual features in both directions are first spliced, and then the channel is compressed using a convolution kernel of 1×1. Subsequently, batch normalization and nonlinear regression are used to encode the spatial information of the two different directions to obtain the attention relation map f_c, i.e:

$$f_c = Conv^{1\times1}\left(concat\left(z_c^h, z_c^w\right)\right) \tag{16}$$

After obtaining the attention relation map, it is successively sliced, 1×1 convolutional transformed and activated by the activation function to obtain the final region weights g_c^h and g_c^w, which are applied to the input features P_c, and the attention-enhanced feature map can be obtained. Where the vertical region weights, horizontal region weights and adjusted features are denoted as:

$$g_c^h = \sigma\left(Conv^{1\times1}\left(f_c^h\right)\right) \tag{17}$$

$$g_c^w = \sigma\left(Conv^{1\times1}\left(f_c^w\right)\right) \tag{18}$$

$$D_c(i, j) = P_c(i, j) \times g_c^h(i) \times g_c^w(j) \tag{19}$$

where f_c^h and f_c^w are two independent tensors after slicing, σ denotes the sigmoid activation function, and D_c is the feature map after attention adjustment.

The new ECA module fusion has the location of the largest sensory field in the backbone network, which can fully capture the global feature information and effectively play the role of the attention mechanism.

3.2.3 Adding a small target detection layer

To tackle the initial issue of challenges in detecting small targets within the complex YOLOv5 framework, this paper incorporates a small target detection layer into the network. During the feature extraction process carried out by the convolutional neural network, the model continuously filters out unhelpful information and low - level semantic details, and keeps high - level semantic information. Nevertheless, when eliminating unhelpful information and low - level semantic details, the model is prone to discarding small targets that take up relatively few pixel points. Even if the model does not eliminate the small targets, the small targets may still disappear from the high-level feature map after multiple downsampling because they contain

fewer pixel points.

To address the issue that the original feature map of YOLOv5 struggles to detect small targets, this research paper introduces a novel small target detection layer at the rear of the network. By performing an up - sampling operation, the size of the feature map in the small target detection layer becomes larger compared to other feature maps. As a result, it can be merged with the shallow feature map. Given that the feature maps at a shallower level possess more abundant details regarding small objects, the spliced feature maps can better detect small targets. Although the added detection layer will significantly increase the training cost of the network, This paper also adds a corresponding detection head alongside a newly - devised small - target detection layer.

Moreover, it will notably enhance the network's ability to detect small targets. This detection head together with the original three detection heads of YOLOv5 form the new network detection head. Since the new small target detection layer generates feature maps of larger size, this new detection head can better handle the detection task of smaller targets, while the original three detection heads can better handle the detection task of larger targets.

3.2.4 Improvement of the loss function

The loss function serves to gauge the extent of error between the model's predicted values and the actual values, significantly mirroring the model's stability performance. In YOLOv5, the loss function is composed of three components. Firstly, there is the classification loss, which is employed to determine whether the anchor box aligns with the corresponding calibrated category. Secondly, the localization loss is used to compute the positional discrepancy between the predicted frame and the actual frame. Lastly, the confidence loss calculates the network's confidence in the prediction of the target. In this research, the CIoU Loss, a type of loss function, is enhanced to enable a more precise calculation of target location information during the fire target detection of electric vehicles on passenger ships. The intersection and merger ratio (IoU) function calculates the ratio of the intersection and merger of two bounding boxes, which is used to measure the accuracy of the prediction box, i.e:

$$IoU = \frac{\left|B \cap B_{gt}\right|}{\left|B \cup B_{gt}\right|} \tag{20}$$

where B, B_{gt} denote the prediction frame and the real frame respectively, usually the higher the value of IoU, the more accurate the prediction frame of the network. However, using the traditional IoU as the loss function, two objects if they do not overlap, the value of the IoU and the gradient are almost 0, which can not reflect the size of the distance between the two, so the function can not be optimized. For this reason YOLOv5 proposes three methods to improve the loss function, which are GloU, DIoU and CIoU.

CIoU is to make improvements on the basis of GloU and DIoU, the convergence speed and the effect of fitting are better than the former, the loss of the size of the detection frame as well as the loss of the length and width are added, which can make the prediction frame more overlap with the real frame, and the convergence speed and the effect of fitting are better than the former. To wit:

$$CIoU = IoU - \left(\frac{\rho^2\left(b, b_{gt}\right)}{d^2} + \alpha\nu \right) \tag{21}$$

The αv is added to the function, where α is the weight coefficient and v is used to measure the consistency of the aspect ratio, defined by Eq:

$$v = \frac{4}{\pi^2}\left(\arctan\frac{w_{gt}}{h_{gt}} - \arctan\frac{w}{h}\right)^2 \tag{22}$$

Building upon the improvement of CIoU, a square - root operation is applied to the Euclidean distance in the partition of Eq. (21). When identifying the quantity of electric vehicles on a passenger ship in a fire situation, images may display scenes of varying sizes. As the target gets larger, the distance between the detection frame and the center point of the actual frame also increases. During the loss calculation, this distance for large targets is notably greater than that for small targets, which is unfavorable for calculating the loss of small targets. Therefore, through the method of opening the square root, the loss weight of the large target can be reduced, and the loss can be calculated more effectively, and it is found through experimental analysis that the computation of the algorithm before and after the improvement of the loss function basically does not increase,Consequently, the computational cost of the model remains unchanged. Incorporating the open square - root results in an enhancement. This enhancement causes the loss value to be lower compared to the pre - improvement state. Moreover, it accelerates the convergence speed of the loss value, thereby enhancing the convergence effect of the loss function. The enhanced loss function is:

$$Loss = IoU - \left(\frac{\sqrt{\rho^2\left(b, b_{gt}\right)}}{d^2} + \alpha v\right) \tag{23}$$

4 Simulation of Fires and Detection of Targets in Electric Vehicles Transported by Roll - on/Roll - off Vessels

In the wake of the advancement and evolution of scientific and technological fields, electric vehicles are increasingly coming into people's lives, becoming another choice after fuel-powered vehicles. Despite the significant enhancement of vehicle battery safety due to technological advancements, fire incidents involving electric vehicles continue to happen intermittently both domestically and internationally. Achieving effective simulation and quantitative evaluation of electric vehicle fires on passenger ships holds great importance in minimizing fire - related losses and safeguarding personal safety.

4.1 Thermal Runaway Simulation of Electric Vehicles Carried by Rolling Stock Vessels

4.1.1 Heat release rate analysis

Drawing on the deck simulation model of the passenger ship transporting electric vehicles that was developed in the preceding section, and then combined with the FDS simulation software and the heat rate calculation formula, we analyze the trend of the heat release rate under the thermal runaway state of the passenger-ship-carrying electric vehicle. Fig. 4 Comparison of HRR curves for the whole vehicle combustion of passenger-roller ship carrying electric vehicles.

As shown in Fig. 4, the simulated HRR curve of electric vehicle full-size combustion is

located between super fast fire and fast fire. Compared with the HRR curve obtained from the full-size actual fire test of fuel car, the simulated heat release rate curve of fuel car fire has the same trend, but the PHRR is lower. The reason may be that the length of the vehicle in this paper is 4.90M, which is slightly shorter than the test vehicle. And in recent years, the material flame retardant technology has also been improved, and the material PHRR has decreased. In addition, the PHRR of the whole vehicle combustion of electric vehicles can reach 29.75MW, which is about 30MW by using the PHRR estimation formula of electric vehicle fire given in the previous section, and the two values are close to each other, with a deviation of only 0.84%.

Considering that the HRR of the whole vehicle combustion has been smaller after 2000s, and the interior combustibles have been burned sufficiently, the first 2000s are selected for analysis. The HRR of the fuel vehicle is larger than that of the electric vehicle in the first 500s, however, the HRR of the electric vehicle is larger than that of the fuel vehicle after 500s. The reason for the difference is that the ignition source fuel fire develops quickly to reach stability, while the battery thermal runaway has an intermittent nature although the behavior of the jet fire is more violent, the total heat release (THR) is still relatively low at the initial stage, and in the middle and late stages, the battery pack reaches the critical temperature to start triggering the thermal runaway and further releases a large amount of heat. The PHRRs of fuel and electric vehicles are 28.03 MW and 29.75 MW, respectively, and the latter reaches the peak with a delay of about 100 s, which is consistent with the trend of the current research for small car fires. The THR of the whole vehicle combustion for fuel and electric vehicles are 18.02 GJ and 20.15 GJ, respectively, and the difference is due to the fact that the power battery of the latter stores more energy.

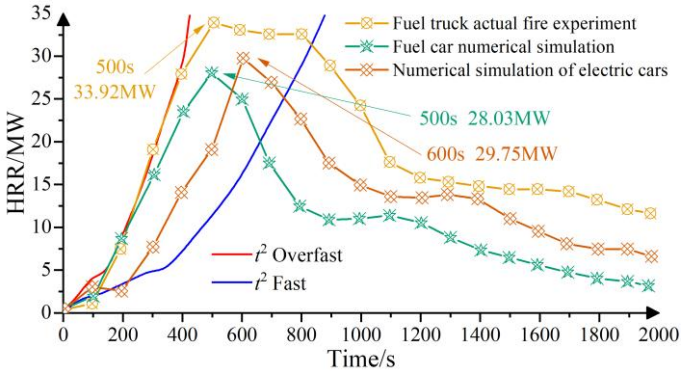

Figure 4: The change in thermal rate 360s before the ignition point

4.1.2 Changes in visibility patterns

In the scenario of a fire in an electric vehicle carried by a passenger ship, the spread of smoke causes visible light to be obscured by smoke particles and weakened, and visibility is rapidly reduced. The visibility of people will be greatly reduced, which seriously affects the escape route of people, and is not conducive to effectively grasp the fire point of the electric car, delaying the fire rescue time and causing greater losses. However, compared with the evacuation of people in the building, the passenger ship due to the transportation of electric vehicles resulting in a smaller space, in the event of a fire, people in the case of unrestricted movement escape basically will not be affected too much, but there is still a need to monitor the visibility of the key points. Therefore, visibility detectors are set up in the front, middle and rear parts of the deck simulation model given before, and 50 and 200 battery pack burning conditions (i.e., conditions A and B) are set up to detect the change rule of visibility in the event of a battery pack fire in a passenger ship carrying an electric vehicle, as shown in Fig. 5.

As can be seen from the figure, the visibility is not affected before the smoke layer is formed

(the first 22 s or so). At the time when the smoke overflowed on the deck, the visibility was rapidly reduced, basically to below 5m in 10s, and rapidly reduced to below 1m. The time for visibility to fall below 0.5m in front, center and aft positions on the deck in Case A is about 27s, 33s and 55s, respectively. In Case B, the time for visibility to drop below 0.5 m in the front, center and aft positions is about 22s, 26s and 32s, respectively. Considering the response time of the personnel to the fire, the evacuation time available for the personnel in the fire scenario of a passenger ship carrying an electric vehicle is less. It can be seen that during the development of the battery pack fire, the visibility inside the deck of the passenger-ship carrying electric vehicle decreases rapidly, and the visibility decreases faster in the front and center positions than in the aft position, and those with a higher chance of escape are the passengers in the aft position of the deck. When the scale of the battery fire is expanded, the visibility reduction rate increases, and there is little difference between the front, middle and aft positions when the visibility drops to the lowest moment. Therefore, the early stage of a fire on a passenger ship carrying an electric vehicle is a critical stage for the escape of personnel, and once the smoke settles inside the deck, the visibility inside the deck will rapidly decrease to a dangerous value.

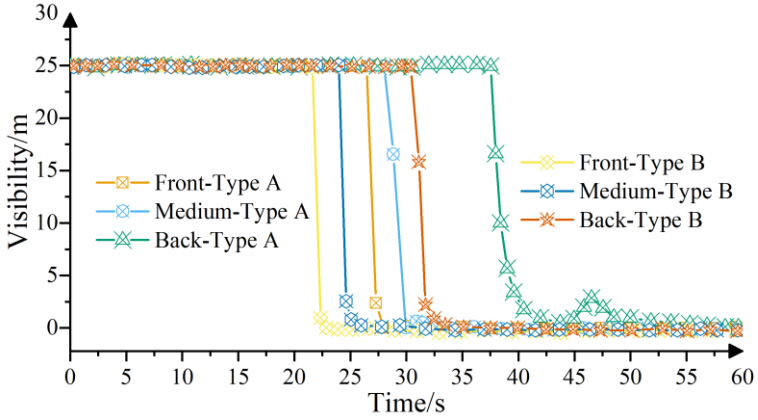

Figure 5: Change laws of visibility

4.1.3 Temperature changes in the region

Figure 6 shows the temperature changes of four classic locations inside the EV, including the battery, the cabin and the front and rear power compartments, when a fire occurs in the EV carried by a passenger ship. The temperature distribution law in the fire scenario is more consistent with the temperature distribution in the actual fire experiment, and the temperature changes are analyzed as follows:

(1) Battery temperature change. In 0~50s, the temperature rises rapidly after ignition, and thermal runaway propagation begins to occur in the interior of the battery pack, but the temperature trend is discontinuous and fluctuates at this time, which is due to the emergence of flames in the cracks. At this time, the battery pack was in a negative ignition state, and the combustion temperature was in the range of 400~600°C. Subsequently, between 50 and 60s, the measured core group further turned to the deflagration state, and the temperature image increased dramatically, and the combustion temperature rapidly reached 1000°C. Then, between 60~100s, the core group detected at the temperature measurement point as well as those in its vicinity gradually subsided, and the temperature began to decrease. Finally, within 100~200s, the sustained high temperature makes the window glass break, the outside gas rushes into the car, the combustible material inside the car starts to burn, the temperature of the measured point rises slightly and finally stabilizes between 780~830°C.

(2) Temperature change in the cabin. between 0~80s, the temperature inside the car gradually increased due to the temperature conduction of thermal runaway of the chassis battery. Then, between 80~120s, with the rupture of the window glass and the entry of external gas into the compartment, the combustible materials inside the car began to burn, and this stage also became the reignition stage, and the measured temperature rose sharply, finally reaching about 900℃. Then, within 140~150s, the combustible materials near the front measurement point were burned out, and the temperature dropped to about 300℃, while the flame inside the car began to spread to the rear row. Finally, between 150~200s, the combustibles in the rear row burned one after another, and the temperature inside the car rose again.

(3) Powerhouse temperature change. Since the thermal runaway trigger position is close to the front of the body, the overall vehicle fire spread shows a trend from front to back. For the front power compartment, between 0 and 100s, affected by the thermal runaway of the chassis battery, the flame spreads from the gap above the battery pack, and the temperature trend in the power compartment is consistent with the trend of burning intensity in the front of the battery pack. During this period, the high temperature caused the electrical equipment and piping in the powerhouse to ignite, and the temperature even reached 700°C. Then, within 100~200s, the temperature inside the powerhouse gradually decreased as the combustion of the cell set in the front part of the battery pack gradually subsided and the flame and heat decreased. For the rear powerhouse, the temperature at the detection point continued to rise in 0~200s. After 175s, the temperature of the rear powerhouse exceeds that of the front, and the rate of increase is further accelerated. Comparing the temperatures of the front and rear powerhouse with the temperature of the compartment, the temperature of the powerhouse was consistently higher than the temperature of the compartment in 0~82s, and the flame spread faster to the powerhouse than to the compartment.

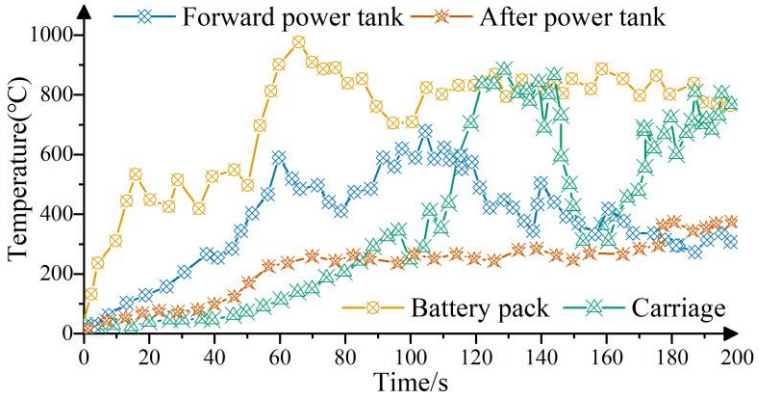

Figure 6: Temperature variations in different areas of the vehicle

4.2 Detection of the target number of combustion targets for the transportation of electric vehicles

4.2.1 Comparison of model performance

In order to verify the superiority of the YOLOv5-ECA model proposed in this paper, the Backbone of YOLOv5 is replaced with the classical lightweight networks CSPDarkNet53-Tiny and MobileNet-v3 for performance comparison. During the experimental test, the same test set is selected and all the test parameters are the same, Table 1 shows the performance index parameters such as mAP, Precision and Recall of different models.

From the table, it can be seen that the improved YOLOv5-ECA model compared with CSPDarkNet53 model, the number of model parameters is 17.83%, the model weights are

reduced by 82.79%, the mAP value is reduced by 0.61%, and the FPS value is improved by 164.48%. It shows that the improved YOLOv5-ECA model is more suitable for target detection in the fire scene of electric vehicles carried on passenger and ro-ro ships, and can realize high-precision real-time monitoring. Compared with the original YOLOv5 model, the number of model parameters increased by only 0.03M, the AP value of smoke target monitoring increased by 4.58%, and the AP value of flame target monitoring increased by 9.79%. The experimental results show that the introduction of the coordinate attention mechanism and the small target detection layer can effectively extract the feature extraction of various types of targets at the fire scene of the electric vehicle carried by the passenger-roller ship, further optimize the detection effect of the electric vehicle in the fire, and help to enhance the YOLOv5-ECA model accuracy.

Table 1: Comparison table of evaluation index parameters of different models

Index	CSPDarkNet53	CSPDarkNet53-Tiny	MobileNet-v3	YOLOv5	YOLOv5-ECA
AP_{fire}	85.74	81.26	75.94	76.53	84.02
AP_{smoke}	92.34	84.81	87.46	88.15	92.19
$F1_{fire}$	0.915	0.865	0.742	0.704	0.814
$F1_{smoke}$	0.947	0.894	0.885	0.869	0.898
mAP/%	88.96	83.06	80.93	82.35	88.42
FPS	28.41	55.38	40.24	76.03	75.14
Weight/M	245.16	22.41	83.78	43.05	42.18
Params/M	64.27	6.06	11.75	11.43	11.46

4.2.2 Detection of target number

Based on the deck simulation model designed in the previous section, we simulate the fire from the middle of the ship, and extract the simulation images at different simulation times (10s~80s), and select different models to carry out the evaluation and detection of the number of targets of electric vehicles, in order to understand the economic losses that may be caused by the fire of the electric vehicles carried by the passenger ship. Table 2 shows the results of target quantity assessment and detection of different models.

As is evident from the table, during the initial 10 seconds of the fire simulation for the electric vehicle being transported by the passenger ship, the detection accuracy of the three models for the number of electric vehicles can reach 100%, which is due to the fact that the fire has just started in 10s, and the overall smoke and flames are small, sThe target detection performance of the three models shows a high degree of consistency. As the fire simulation time progresses, the detection accuracy of both the CSPDarkNet53 model and the YOLOv5 model declines. Similarly, the detection accuracy of the YOLOv5 - ECA model developed in this study also decreases. However, the overall reduction in the detection accuracy of the YOLOv5 - ECA model is notably less than that of the comparison models. Moreover, the model presented in this paper is more effective at distinguishing the characteristics of smoke and flame. , so as to exclude the cars burned by the flame from the number of normal electric vehicles, which provides more accurate data for analyzing the economic loss of electric vehicles affected by fire. Therefore, Leveraging the target detection model can efficiently achieve an accurate evaluation of the quantity of electric vehicles transported by passenger and roll - on/roll - off vessels in fire situations. Moreover, it can offer dependable decision - making support for formulating fire safety measures for the electric vehicles carried by these vessels.

Table 2: Comparison of prediction results of different models

Time/s	Actual value	CSPDarkNet53	YOLOv5	YOLOv5-ECA
10	240	240	240	240
20	220	230	228	220
30	190	200	198	189
40	170	182	179	171
50	150	163	160	152
60	120	131	129	124
70	100	118	115	104
80	90	109	104	95

5 Conclusion

In this article, an FDS numerical simulation tool is employed to construct a fire dynamics model for electric vehicles (EVs) transported on a passenger ship. Subsequently, a thermal runaway simulation analysis is conducted. The coordinate attention mechanism is then integrated with the YOLOv5 model to develop a target quantity detection model, which is used to assess the variation in the number of EVs during fire incidents.It has been discovered that the peak heat release rate (PHRR) during the combustion of an entire EV can reach up to 29.75 megawatts. This value shows a deviation of only 0.84% from the actual calculated PHRR. There are disparities in the temperature fluctuations at different positions of the EVs. These temperature changes can be utilized to pinpoint the specific location on the passenger ship where the EVs are being carried when a fire breaks out.By leveraging the YOLOv5 - ECA model, it is possible to achieve highly efficient detection of the fire situation of EVs on passenger - roll on/roll off ships. This model also offers reliable data support for analyzing the economic losses of EVs resulting from fires.

References

[1] Brzezinska, D., & Bryant, P. (2022). Performance-based analysis in evaluation of safety in car parks under electric vehicle fire conditions. Energies, 15(2), 649.

[2] Sun, P., Bisschop, R., Niu, H., & Huang, X. (2020). A review of battery fires in electric vehicles. Fire technology, 56(4), 1361-1410.

[3] Węglarz, K., Złoczowska, E., & Krasuski, A. (2024). Problems of fire protection in the Ro-ro space of roll-on/roll-off ships during an electric vehicle fire Part 1 problem areas in fire protection of cargo decks of Ro-ro ships in the context of an electric vehicle fire. Scientific Reports of Fire University, 1(90), 109-129.

[4] Jiang, X., Ren, W., Xu, H., Zheng, S., & Wu, S. (2025). Mechanism-Based Fire Hazard Chain Risk Assessment for Roll-On/Roll-Off Passenger Vessels Transporting Electric Vehicles: A Fault Tree–Fuzzy Bayesian Network Approach. Journal of Marine Science & Engineering, 13(2).

[5] Ouyang, D., Liu, J., Chen, M., & Wang, J. (2017). Investigation into the fire hazards of lithium-ion batteries under overcharging. Applied Sciences, 7(12), 1314.

[6] Ghiji, M., Novozhilov, V., Moinuddin, K., Joseph, P., Burch, I., Suendermann, B., & Gamble, G. (2020). A review of lithium-ion battery fire suppression. Energies, 13(19), 5117.

[7] Chow, W. K., & Chow, C. L. (2022). Electric vehicle fire hazards associated with batteries, combustibles and smoke. International Journal of Automotive Science and Technology, 6(2), 165-171.

[8] Arvidson, M., Gehandler, J., & Bleye, J. (2023). Fire suppression and manual firefighting of battery electric vehicle fires on ro-ro ships. In de Proceedings from the Seventh International Conference on Fire in Vehicles, Borås, RI. SE (pp. 107-118).

[9] Almeida, J. A. G., Medina, F. H. H., de Ganzo, M. D. C. A., Correa, A. U. G., & de Luz, J. A. (2023). Transport of Electric and Hybrid Vehicles on Board Ships: Risks and Measures to Consider for a Growing Problem. Journal of Maritime Research, 20(3), 240-250.

[10] Lin, J. Q., & Kuo, S. Y. (2024, October). Risk Management Strategies for Electric Vehicles in Maritime Transportation. In 2024 IEEE 13th Global Conference on Consumer Electronics (GCCE) (pp. 290-291). IEEE.

[11] Mubarok, A. (2024). Risk Mitigation For Ship Cargo And Electric Vehicle Cargo In Ferry Transportation. Journal of Education and Technology Development, 2(1), 60-74.

[12] Yu, Y., Zhang, J., Yin, H., & Zhang, W. (2025). Study on Fire Evolution Simulation of Zoning Strategy for Battery Electric Vehicles in RoPax Ship. IEEE Transactions on Transportation Electrification.

[13] Bao, J., Bian, Z., Li, B., Li, Y., & Gong, Y. (2023). A hybrid approach for quantitative analysis of fire hazards in enclosed vehicle spaces on ro-ro passenger ships. Sustainability, 15(17), 13059.

[14] Kim, K., & Jeon, H. (2023). The causes and responses to cargo hold fire accidents in RoRo ships using AcciMap. Journal of International Maritime Safety, Environmental Affairs, and Shipping, 7(4), 2274227.

[15] Xie, X. I. A. O. D. O. N. G., Liu, N. A. I. A. N., Viegas, D. X., & Raposo, J. R. (2014). Experimental research on upslope fire and jump fire. Fire Safety Science, 11, 1430-1442.

[16] Li, T., Zhao, W., Yuan, J., Wei, X., Zhao, J., & Yang, X. (2025). Prediction of heat release rates from lithium-ion battery fires: A methodology incorporating digital imaging and experimental analysis. Journal of Energy Storage, 137, 118645.

[17] McGrattan, K., Hostikka, S., McDermott, R., Floyd, J., Weinschenk, C., & Overholt, K. (2013). Fire dynamics simulator user's guide. NIST special publication, 1019(6), 1-339.

[18] Rahmani, A., & Salem, M. (2020). Simulation of fire in super high-rise hospitals using fire dynamics simulator (FDS). Electronic Journal of General Medicine, 17(3), 5.

[19] Floyd, J., & Madrzykowski, D. (2024). Fire dynamics simulator modeling of a line-of-duty death in a firefighting training facility using recent research on materials and firefighter safety. Journal of Fire Sciences, 42(3), 248-278.

[20] Lee, J., Kim, B., Lee, S., & Shin, W. G. (2023). Validation of the fire dynamics simulator (FDS) model for fire scenarios with two liquid pool fires in multiple compartments. Fire Safety Journal, 141, 103892.

[21] Tzani, M., Besharat, J., Charalampous, V., & Stylios, C. (2020, September). Building a virtual reality fire environment based on fire dynamic simulator. In 2020 International Conference on Information Technologies (InfoTech) (pp. 1-5). IEEE.

[22] Kang, D. I., Kim, K., Jang, S. C., & Yoo, S. Y. (2015). Risk assessment of main control board fire using fire dynamics simulator. Nuclear Engineering and Design, 289, 195-207.

[23] Enaru, I., Chereches, N. C., Hudișteanu, S. V., Țurcanu, E. F., Ancas, A. D., Verdeș, M., ... & Ciocan, V. (2023). Numerical simulation evaluation of fire spreading in a building using fire dynamics simulator (FDS). Journal of Applied Engineering Sciences, 13(1), 65-72.

[24] Huang, Y. H. (2022). Using Fire Dynamics Simulator to reconstruct a fire scene in a hospital-based long-term care facility. Journal of Loss Prevention in the Process Industries, 80, 104863.

[25] Mirahadi, F., McCabe, B., & Shahi, A. (2019). IFC-centric performance-based evaluation of building evacuations using fire dynamics simulation and agent-based modeling. Automation in Construction, 101, 1-16.

[26] Valasek, L., & Glasa, J. (2017). On realization of cinema hall fire simulation using Fire Dynamics Simulator. Computing and Informatics, 36(4), 971-1000.

[27] Zhao, Y., Chen, W., Guo, J., Bao, J., Wu, Y., Ai, D., & Wang, Q. (2025). Fire Simulation and Optimization of Fire Control System in Vehicle Compartment of Ro-Ro Passenger Ship. Fire, 8(11), 443.

[28] Ji, J., Ma, Z., He, J., Xu, Y., & Liu, Z. (2020). Research on risk evaluation and dynamic escape path planning algorithm based on real-time spread of ship comprehensive fire. Journal of Marine Science and Engineering, 8(8), 602.

[29] Ayci, T., Barlas, B., & Olcer, A. I. (2021). Evaluation on fire incident of electric vehicle spaces onboard ferries with using fire dynamics simulations. Journal of Thermal Engineering, 11(2), 434-447.

[30] Pitana, T., Soewirjo, M. K. Y., Siswantoro, N., & Nurwahyudy, A. (2025). Simulation of an electric vehicle fire on a Ro-Ro Ferry. Journal of Applied Engineering Science, 23(1), 45-54.